Designing OCDM-based Multi-user Transmissions

Muhammad Shahmeer Omar and Xiaoli Ma
School of Electrical and Computer Engineering, Georgia Institute of Technology, Atlanta, GA 30332
Email: {momar6, xiaoli}@gatech.edu

***Abstract*—Orthogonal chirp division multiplexing (OCDM) is a fairly new multi-carrier scheme that employs the discrete Fresnel transform (DFnT) to digitally modulate data onto orthogonal chirps. Most work surrounding OCDM has been done in the context of optical networks and single user wireless systems. Hence, there is no literature regarding multiple access in OCDM. This paper introduces a novel data multiplexing technique that leverages the properties of the DFnT to independently process smaller sub-blocks, thus enabling multiple access and low complexity equalization. Additionally, this paper employs a joint multi-user processing technique and compares its performance to the proposed scheme.**

***Index Terms*—Orthogonal chirp division multiplexing, OFDM, multiple-access, precoding, diversity.**

I. Introduction

Wireless multicarrier techniques such as orthogonal frequency domain multiplexing (OFDM) are vastly popular due to low complexity, high spectral efficiency, robustness to frequency selective channels, etc. Orthogonal chirp division multiplexing (OCDM) is a relatively new scheme which modulates data onto orthogonal chirps [1]–[4].

Digital implementations of OCDM, introduced in [1]–[2], employ the discrete Fresnel transform (DFnT) in the baseband, much like OFDM employs the discrete Fourier transform (DFT). In [1], it is shown that while having identical peak to average power as OFDM, OCDM showed improved bit error rate (BER) performance and greater resistance to interference caused by insufficient guard lengths. The study in [2] analyzed the performance of OCDM in coherent optic fiber networks, [3] experimentally showed optical data rates of up to a 112 Gbps using OCDM and intensity modulation with direct detection and [4] used a combination of experiments and simulations to analyze the performance of OCDM for millimeter wave fiber wireless systems. An orthogonal chirp spread spectrum (CSS) technique is investigated in [5] and it is shown that an arbitrary number of chirps can be multiplexed to achieve the Nyquist rate. In [6], the performance of orthogonal frequency division multiple access (OFDMA) in doubly selective uplink channels is analyzed and an iterative equalizer is proposed to mitigate multiple access interference.

Linear constellation precoding (LCP) has been proposed to exploit maximum diversity and coding gains in single antenna OFDM systems [7]–[8], and for multi-antenna systems in conjunction with space-time coding in [9]–[10]. In [7], grouped carrier LCP (GLCP) OFDM has been proposed to get maximum diversity and coding gains while decreasing equalization complexity. Precoding strategies for space-time coded systems were outlined and analyzed in [9]–[10] with the objective of exploiting both multipath and antenna diversity, resulting in significant performance enhancement. The diversity and coding gain performance of single carrier with cyclic prefix (SC-CP) systems has been analyzed in [11] and shown to be dependent on the block size, constellation and the signal to noise ratio (SNR).

To the best of the authors knowledge, multi-user OCDM has not been studied so far. Most work surrounding OCDM has either focused on single user wireless links or optical networks. Moreover, constellation precoding for OCDM has not been investigated either. The primary goal of this paper is to propose and develop a symbol multiplexing technique that applies GLCP to OCDM as well as frequency domain equalization for orthogonal chirp division multiple access (OCDMA). For comparison, we also analyze the performance of the joint detection technique in [6] for multi-user detection in OCDMA.

Common notations used in this study include upper case bold letters, like $\mathbf{A}$, and lower case bold letters, like $\mathbf{a}$, for matrices and vectors, respectively. $\mathbf{A}^{\mathcal{H}}$, $\mathbf{A}^T$ denote the conjugate transpose and transpose of $\mathbf{A}$, respectively and $\|\mathbf{a}\|$ denotes the l_2 norm of a vector $\mathbf{a}$. In general the $P \times P$ DFT matrix is given by $[\mathbf{F}_P]_{k,n} = 1/\sqrt{P}\ e^{-j2\pi nk/P}$. However, wherever the size of the DFT matrix is $N \times N$, where N is the block length, the subscript is omitted.

II. System Model

Consider OCDM transmissions over frequency selective fading channels. A serial stream of QAM symbols is grouped into blocks of size N and the i-th block is given by $\mathbf{u}(i) = [u(iN), u(iN+1)...u(iN+N-1)]^T$. The symbols are linearly precoded to give $\mathbf{s}(i) = \mathbf{\Lambda u}(i)$, where $\mathbf{\Lambda}$ denotes the precoder matrix. The symbols are then modulated onto orthogonal chirp signals by computing the IDFnT. The DFnT matrix $\mathbf{\Phi}$ is given by

$$\Phi(m,n) = \frac{1}{\sqrt{N}} e^{-j\frac{\pi}{4}} \times \begin{cases} e^{j\frac{\pi}{N}(m-n)^2} & N \equiv 0 \text{ (mod 2)} \\ e^{j\frac{\pi}{N}(m+\frac{1}{2}-n)^2} & N \equiv 1 \text{ (mod 2)}. \end{cases} \tag{1}$$

In order to facilitate low complexity implementation, the fast Fourier transform (FFT) algorithm can be used in conjunction with the decomposition $\mathbf{\Phi} = \mathbf{\Theta}_2\mathbf{F}\mathbf{\Theta}_1$, as shown in [1]–[2]. A cyclic prefix (CP) of length L is added to the block, before being serialized, pulse shaped and transmitted.

This work is, in part, supported by a Industry/University Cooperative Research program of National Science Foundation Center of Fiber Wireless Integration and Networking (FiWIN) for heterogeneous mobile data communications under contract number 1539976.

For the purpose of this study, we assume that the CP length is sufficient to avoid inter block interference (IBI). Hence the channel is modeled as a length $L+1$ FIR filter $\mathbf{h} = [h(0),\ ...,\ h(L)]^T$ with each tap being an independent zero mean complex Gaussian random variable with variance $1/(L+1)$. This corresponds to the assumption of Rayleigh fading. Furthermore, we assume that the channel is quasi-static, i.e., it does not vary over the period of one block but changes in between blocks. For simplicity, we primarily use notations consistent with single user scenario in this section. However, the model can easily be extended to multi-user systems.

At the receiver, the received symbols are amplified, filtered and converted into blocks. Assuming perfect time and frequency synchronization, the received symbol block, after deleting the CP, is given by

$$\mathbf{x}(i) = \tilde{\mathbf{H}}\mathbf{\Phi}^{\mathcal{H}}\mathbf{s}(i) + \mathbf{n}(i), \tag{2}$$

where $\mathbf{n}(i)$ represents the additive white Gaussian noise and $\tilde{\mathbf{H}}$ is a circulant matrix, whose first column is given by $[\mathbf{h}^T\ \mathbf{0}_{N-L-1}^T]^T$, as is the case for any scheme that employs CP [12]. Given that the system has no memory, i.e., the current block is independent of previous blocks, we will drop the block index i from this point on without losing generality. After removing the CP, the symbols are demodulated, equalized and sent for detection.

III. Frequency Shift Precoding

In this section we introduce frequency shift precoding (FSP) as a method to multiplex symbols such that they can be independently processed in the frequency domain at the receiver. As will be shown in the following sections, this allows for low complexity maximum likelihood equalization (MLE) and multi-user processing in the frequency domain. It is pertinent to note here that the technique itself is similar to the one used in interleaved frequency division multiple access (IFDMA), proposed in [14]. However, IFDMA is shown as an alternative to frequency division multiple access (FDMA) for single carrier systems, but this paper uses FSP to overcome interference caused by the frequency selective channel in OCDM.

Let us assume there are M blocks of K symbols, such that the aggregated number of symbols is given by $N = MK$, that need to be transmitted. In order to develop FSP, we rewrite Eq. (2) to get

$$\mathbf{x} = \mathbf{F}^{\mathcal{H}}\mathbf{D}_h\mathbf{\Gamma}^{\mathcal{H}}\mathbf{F}\mathbf{s} + \mathbf{n}, \tag{3}$$

where $\mathbf{D}_h$ and $\mathbf{\Gamma}$ are diagonal matrices with the channel frequency response and the root Zadoff-Chu sequence, given by Eq. (4), on the main diagonal, respectively.

$$\Gamma(k,k) = \begin{cases} e^{-j\frac{\pi}{N}k^2} & N \equiv 0 \pmod 2 \\ e^{-j\frac{\pi}{N}(k^2-k)} & N \equiv 1 \pmod 2. \end{cases} \tag{4}$$

This follows from the eigenvalue decomposition $\mathbf{\Phi} = \mathbf{F}^{\mathcal{H}}\mathbf{\Gamma}\mathbf{F}$. Converting the input symbols to the frequency domain, and multiplying with $\mathbf{\Gamma}$, obtain

$$\begin{aligned} \tilde{\mathbf{x}} = \mathbf{\Gamma}\mathbf{F}\mathbf{x} &= \mathbf{\Gamma}\mathbf{D}_h\mathbf{\Gamma}^{\mathcal{H}}\mathbf{F}\mathbf{s} + \mathbf{\Gamma}\mathbf{F}\mathbf{n} \\ &\overset{(a)}{=} \mathbf{D}_h\mathbf{F}\mathbf{s} + \mathbf{\Gamma}\mathbf{F}\mathbf{n}, \end{aligned} \tag{5}$$

where the equality (a) follows from the commutative property of two diagonal matrices and the definition of $\mathbf{\Gamma}$. Eq. (5) shows that in order to avoid interference among the M transmitted blocks, the location of the zeros in the frequency domain symbols $\mathbf{F}\mathbf{s}$ need to be controlled. In the subsequent lemma we leverage the properties of the DFT to devise a method to introduce these zeros.

Lemma 1: Given a length-K time domain sequence $v(n)$ with a K-point DFT given by $V(k)$, where $K = 2^l$ and $l \geq 1$, the N-point DFT of the periodic extension of the signal $\tilde{v}(n)$, created by repeating v, M times, is given by

$$\tilde{V}(k) = \begin{cases} \sqrt{M}V\left(\frac{k}{M}\right) & \text{if } \frac{k}{M} \in \mathbb{Z}^+ \\ 0 & \text{elsewhere,} \end{cases} \tag{6}$$

where $\mathbb{Z}^+$ denotes the set of non-negative integers.

Proof: The N point DFT of the extended signal is given by

$$\begin{aligned} \tilde{V}(k) &= \frac{1}{\sqrt{N}}\sum_{n=0}^{N-1}\tilde{v}(n)e^{-j\frac{2\pi kn}{N}} \\ &= \frac{1}{\sqrt{N}}\sum_{l=0}^{M-1}\sum_{n=lK}^{(l+1)K-1} v(n-lK)e^{-j\frac{2\pi kn}{N}}. \end{aligned}$$

Introducing the substitutions $n' = n - lK$ and $N = MK$ gives us

$$\tilde{V}(k) = \underbrace{\left(\frac{1}{\sqrt{M}}\sum_{l=0}^{M-1}e^{-j\frac{2\pi kl}{M}}\right)}_{(a)}\left(\frac{1}{\sqrt{K}}\sum_{n'=0}^{K-1}v(n')e^{-j\frac{2\pi n'}{K}(\frac{k}{M})}\right). \tag{7}$$

It is well established that the expression (a) in Eq. (7) simplifies to $\sqrt{M}\sum_{i=0}^{K-1}\delta(k-iM)$, where $\delta(.)$ is the Dirac-delta function i.e., $\delta(0) = 1$ and $\delta(k) = 0$ for $k \neq 0$. Substituting this into Eq. (7) gives us

$$\begin{aligned} \tilde{V}(k) &= \sqrt{M}\sum_{i=0}^{K-1}\delta(k-iM)\left(\frac{1}{\sqrt{K}}\sum_{n'=0}^{K-1}v(n')e^{-j\frac{2\pi n'}{K}(\frac{k}{M})}\right) \\ &= \sqrt{M}\sum_{i=0}^{K-1}\delta(k-iM)V\left(\frac{k}{M}\right), \end{aligned} \tag{8}$$

which completes the proof.

Lemma 1 shows that periodic extension of a length K signal to a length N signal is equivalent to adding $M-1$ zeros between the original DFT samples. Subsequently, multiplexing multiple blocks simply then becomes a question of shifting each block by a variable amount in the frequency domain which leads into the following theorem.

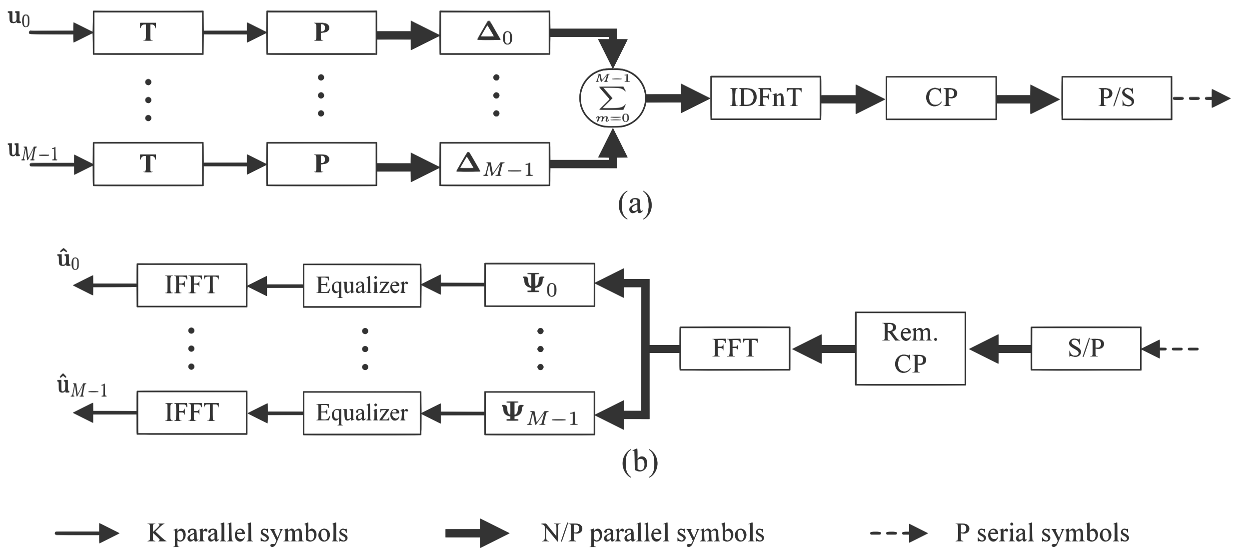

Fig. 1. FSP transmitter (a) and receiver (b). The time domain symbol estimates are given by $\hat{\mathbf{u}}_m$.

Theorem 1: Shifting the frequency domain sequences $\tilde{V}(k)$ by an integer m, where $m = [0, M-1]$ allows for the multiplexing of a maximum of M length K sequences without interference.

Proof: The proof for this is fairly trivial and can be directly seen from the fact that $\sum_n \delta(n-m)\delta(n-l) = 0,\ \forall\ m \neq l$.

It is well known that a frequency shift is equivalent to a point-wise multiplication with a fixed frequency tone in the time domain. Hence we represent the FSP for the m^{th} sub-block as the cascade of two precoders $\mathbf{\Lambda}_m = \mathbf{\Delta}_m \mathbf{P}$, given by

$$\mathbf{P} = \frac{1}{\sqrt{M}} [\underbrace{\mathbf{I}_K\ \mathbf{I}_K\ ...\ \mathbf{I}_K}_{M\ \text{times}}]^T$$

$$\mathbf{\Delta}_m(n,k) = \begin{cases} e^{j\frac{2\pi m}{N}n} & \text{when } n = k \\ 0 & \text{otherwise,} \end{cases} \tag{9}$$

where $\mathbf{P}$ is an $N \times K$ matrix, with the scaling factor introduced to maintain constant power, and $\mathbf{\Delta}_m$ is an $N \times N$ diagonal matrix. Hence, given M length K symbols $\mathbf{u}_m$, we can see that

$$\mathbf{s} = \sum_{m=0}^{M-1} \mathbf{s'}_m = \sum_{m=0}^{M-1} \mathbf{\Delta}_m \mathbf{P} \mathbf{u}_m. \tag{10}$$

In order to develop the FSP receiver, we define a $K \times N$ permutation matrix $\mathbf{\Psi}_m$ as

$$\Psi_m(i,l) = \begin{cases} 1 & \text{for } i = 1, ..., K \text{ and } l = 1 + m + M(i-1) \\ 0 & \text{otherwise.} \end{cases} \tag{11}$$

According to Theorem 1, the DFT of the transmitted symbols can then be denoted by $\mathbf{F}\mathbf{s} = \mathbf{F}\sum_{m=0}^{M-1} \mathbf{s'}_m = \sum_{m=0}^{M-1} \mathbf{\Psi}_m^T \mathbf{F}_K \mathbf{u}_m$. Hence, the m^{th} received sub-block is given by

$$\tilde{\mathbf{x}}_m = \mathbf{\Psi}_m \mathbf{D}_h \mathbf{F}\mathbf{s} + \mathbf{\Psi}_m \mathbf{\Gamma}\mathbf{F}\tilde{\mathbf{n}}. \tag{12}$$

Noting that $\mathbf{F}\mathbf{s} = \sum_{l=0}^{M-1} \mathbf{\Psi}_l^T \mathbf{F}_K \mathbf{u}_l$, and that for any $N \times N$ diagonal matrix $\mathbf{D}$, $\mathbf{\Psi}_m \mathbf{D} \mathbf{\Psi}_n^T = \mathbf{0}_{K\times K}\ \forall n \neq m$, Eq. (12) can be rewritten as

$$\begin{aligned} \tilde{\mathbf{x}}_m &= \mathbf{\Psi}_m \mathbf{D}_h \sum_{l=0}^{M-1} \mathbf{\Psi}_l^T \mathbf{F}_K \mathbf{u}_l + \hat{\mathbf{n}}_m \\ &= \mathbf{\Psi}_m \mathbf{D}_h \mathbf{\Psi}_m^T \mathbf{F}_K \mathbf{u}_l + \hat{\mathbf{n}}_m \\ &= \mathbf{D}_{h,m} \mathbf{F}_K \mathbf{u}_m + \hat{\mathbf{n}}_m, \end{aligned} \tag{13}$$

where $\mathbf{D}_{h,m} = \mathbf{\Psi}_m \mathbf{D}_h \mathbf{\Psi}_m^T = \text{diag}(H(m)...H(m + (K-1)M))$, $H(k)$ denotes the frequency response in the k^{th} bin, and $\hat{\mathbf{n}}_m = \mathbf{\Psi}_m \mathbf{\Gamma}\mathbf{F}\tilde{\mathbf{n}}$. For simplicity, we have assumed a single channel $\mathbf{D}_h$ but in later sections, we show that multiple, independent channels do not necessitate any changes in the system. The block diagram for an FSP transceiver is shown in Fig. 1.

IV. Grouped Carrier Linear Constellation Precoding

We have already seen that by using FSP, we are able to partition OCDM symbols into non-intersecting sub-blocks of length $K < N$ in the frequency domain, as shown in Eq. (13). This allows us to apply GLCP to OCDM to achieve maximum coding and diversity gains while reducing MLE complexity. Hence, in this section, we build on the analyses presented in [7]–[11] to show that OCDM with FSP does indeed stand to benefit from the application of GLCP. Prior to further analyses, it is pertinent to note that we have not discussed how a length N block is divided into length K sub-blocks prior to the application of FSP. For the purpose of this study, we simply assume that contiguous K symbols in the block form one sub-block.

In order to apply an LCP, we alter Eq. (13) slightly to get

$$\tilde{\mathbf{x}}_m = \mathbf{D}_{h,m} \mathbf{F}_K \mathbf{T} \mathbf{u}_m + \hat{\mathbf{n}}_m, \tag{14}$$

where $\mathbf{T}$ is the $K \times K$ precoder matrix and $\mathbf{T} = \mathbf{I}_K$ accounts for the unprecoded case. In terms of the design, this precoder precedes $\mathbf{\Lambda}$. Hence, no changes need to be made to the FSP. We use the bound on the conditional pairwise error probability (PEP), given by

$$\mathbb{P}(\tilde{\mathbf{u}}_m \rightarrow \tilde{\mathbf{u}}'_m|\mathbf{h}) \leq \exp\bigg[-\frac{d^2(\tilde{\mathbf{x}}'_m, \tilde{\mathbf{x}}_m)}{4N_0}\bigg],$$

to analyze the performance of MLE, where $d^2(\tilde{\mathbf{x}}'_m, \tilde{\mathbf{x}}_m) = \|\tilde{\mathbf{x}}'_m - \tilde{\mathbf{x}}_m\|^2$. Making use of the substitution from Eq. (14), it is easy to see that $d^2(\tilde{\mathbf{x}}'_m, \tilde{\mathbf{x}}_m) = \|\mathbf{D}_{h,m}\hat{\mathbf{e}}_m\|^2 = \|\mathbf{D}_e\tilde{\mathbf{h}}_m\|^2$, where $\hat{\mathbf{e}}_m = \mathbf{F}_K\mathbf{T}\mathbf{e}_m$, $\mathbf{e}_m = \mathbf{u}'_m - \mathbf{u}_m$, $\mathbf{D}_e = diag(\hat{\mathbf{e}}_m)$, and $\tilde{\mathbf{h}}_m = [H(m),\ H(m+M),\ ...H(m+(K-1)M)]^T$. A vector of i.i.d. fading samples $\bar{\mathbf{h}}$ can be obtained using the relation $\mathbf{h} = \mathbf{B}\bar{\mathbf{h}}$, where $\mathbf{B}\mathbf{B}^{\mathcal{H}} = \mathbf{R}_h$ and $\mathbf{R}_h$ is the channel correlation matrix, which is positive definite. It subsequently follows that $\tilde{\mathbf{h}}_m = \mathbf{\Psi}_m\mathbf{V}_N\mathbf{B}\bar{\mathbf{h}}$, where $\mathbf{V}_N = [\mathbf{v}(0),\ ...,\ \mathbf{v}(N-1)]^T$ is the truncated FFT matrix, $\mathbf{v}(n) = [1, \omega^n,\ ...,\ \omega^{nL}]^T$ and $\omega = \exp(-j2\pi/N)$. For simplicity, we make the substitution $\mathbf{U}_m = \mathbf{\Psi}_m\mathbf{V}_N$, which becomes

$$\mathbf{U}_m = \begin{bmatrix} 1 & \omega^{m} & \dots & \omega^{mL} \\ 1 & \omega^{(m+M)} & \dots & \omega^{(m+M)L} \\ \vdots & \vdots & \ddots & \vdots \\ 1 & \omega^{(m+(K-1)M)} & \dots & \omega^{(m+(K-1)M)L} \end{bmatrix}. \quad (15)$$

Hence, making the appropriate substitutions, we get $\|\mathbf{D}_e\tilde{\mathbf{h}}_m\|^2 = \bar{\mathbf{h}}^{\mathcal{H}}\mathbf{C}_e\bar{\mathbf{h}}$, where $\mathbf{C}_e = \mathbf{B}^{\mathcal{H}}\mathbf{A}_e\mathbf{B}$, and $\mathbf{A}_e = \mathbf{U}_m^{\mathcal{H}}\mathbf{D}_e^{\mathcal{H}}\mathbf{D}_e\mathbf{U}_m$. It is well known that the average PEP, at high SNR, is bounded by

$$\mathbb{P}(\tilde{\mathbf{u}}_m \rightarrow \tilde{\mathbf{u}}'_m) \leq \bigg(G_{c,e}\frac{1}{N_0}\bigg)^{-G_{d,e}},$$

where $G_{d,e} = \mathcal{R}(\mathbf{C}_e)$ is the multipath diversity gain and $G_{c,e} = (\prod_{l=0}^{\mathcal{R}(\mathbf{C}_e)-1}\lambda_l)^{1/\mathcal{R}(\mathbf{C}_e)}$ is the coding gain and λ_l is the l^{th} non-zero eigenvalue of $\mathbf{C}_e$. Due to the fact that we draw the input symbols from a finite alphabet, there are a finite number of possible $\mathbf{e}_m$. As a consequence, we define the coding and diversity gains as

$$G_d = \min_{\forall \mathbf{e}_m \neq \mathbf{0}} G_{d,e} \ \text{ and } \ G_c = \min_{\forall \mathbf{e}_m \neq \mathbf{0}} G_{c,e}, \quad (16)$$

respectively. It is obvious that in order to exploit maximum diversity, $K \geq L+1$ to ensure that $\mathbf{C}_e$ is full rank. Recalling that $N = 2^l$ and $K = 2^n$, where $l > n > 1$ due to the design of FSP, in order to get maximum diversity and coding gains, the system must be designed so that $K = \lceil L+1 \rceil_2$, where $\lceil . \rceil_2$ denotes the closest exponent of 2 that is larger than the argument.

A. Diversity Gain

It is easy to see, from Eq. (16), that $G_d = \min_{\forall \mathbf{e}_m \neq \mathbf{0}} \mathcal{R}(\mathbf{C}_e)$. The dimensions of $\mathbf{C}_e$ thus suggest that the maximum diversity order is given by $G_{d,\text{max}} = L+1$ when $K \geq L+1$, as shown in [7]–[8]. Let us define the matrix $\hat{\mathbf{T}} = \mathbf{F}_K\mathbf{T}$, whose rows (columns) are given by $\hat{\mathbf{t}}_i$ ($\hat{\bar{\mathbf{t}}}_i$) $\forall i \in [1, K]$ and $trace(\hat{\mathbf{T}}^{\mathcal{H}}\hat{\mathbf{T}}) = K$ to preserve power. In order to show that the proposed grouping scheme allows for maximum diversity, we enforce the following condition on our precoder

$$\hat{\mathbf{t}}_i(\mathbf{u}'_m - \mathbf{u}_m) \neq 0 \ \forall i \in [1, K] \text{ and } \forall \mathbf{u}'_m \neq \mathbf{u}_m. \quad (17)$$

Now recall $\mathbf{C}_e = \mathbf{B}^{\mathcal{H}}\mathbf{A}_e\mathbf{B}$, and that $\mathbf{B}$ is always full rank. From the condition in (17), it is easy to see that $\mathbf{D}_e^{\mathcal{H}}\mathbf{D}_e = diag(|\hat{\mathbf{t}}_1\mathbf{e}|^2,\ ...,\ |\hat{\mathbf{t}}_K\mathbf{e}|^2)$ is positive definite. Hence, using the definition of $\mathbf{U}_m$, it follows that $\mathbf{A}_e = \mathbf{U}_m^{\mathcal{H}}\mathbf{D}_e^{\mathcal{H}}\mathbf{D}_e\mathbf{U}_m$ is positive definite and $G_{d,\text{max}} = \min(L+1, K)$.

When there is no precoding, i.e. $\mathbf{T} = \mathbf{I}_K$, the diversity becomes a function of K due to the finite alphabet property [11]. Since, $K \ll N$, we will observe a performance degradation in uncoded and grouped transmissions as the probability of $\hat{\mathbf{e}}_m$ having multiple zero entries increases.

B. Coding Gain

Assuming $\mathbf{C}_e$ is positive definite, the coding gain is given by

$$G_c = det(\mathbf{R}_h)^{1/(L+1)} \underbrace{\min_{\forall \mathbf{e}_m \neq \mathbf{0}} det(\mathbf{U}_m^{\mathcal{H}}\mathbf{D}_e^{\mathcal{H}}\mathbf{D}_e\mathbf{U}_m)}_{(a)}{}^{1/(L+1)}. \quad (18)$$

Using Cauchy-Binet Theorem in [13], (a), in Eq. (18), can be rearranged as $\min\sum_i |det(\tilde{\mathbf{D}}_e^{(i)}\tilde{\mathbf{U}}_m^{(i)})|^2$, where the sum is taken over all matrices obtained by deleting $K-L-1$ rows and $K-L-1$ rows and columns from $\mathbf{U}_m$ and $\mathbf{D}_e$, respectively. It is fairly simple to see that the above sum can be bounded as $G_c \geq \big(\sum_i |det(\tilde{\mathbf{U}}_m)|^2\big)\min|det(\tilde{\mathbf{D}}_e)|^2 = det(\mathbf{U}_m^{\mathcal{H}}\mathbf{U}_m)\min\prod_{j\in\mathcal{I}}|\hat{\mathbf{t}}_j(\mathbf{u}'_m - \mathbf{u}_m)|^2$, where $\mathcal{I}$ is the set of $(L+1)$ rows taken from $\hat{\mathbf{T}}$. Using the fact that $det(\mathbf{U}_m^{\mathcal{H}}\mathbf{U}_m) = K^{(L+1)}$, and $\min\prod_{j\in\mathcal{I}}|\hat{\mathbf{t}}_j(\mathbf{u}'_m - \mathbf{u}_m)|^2 \geq (d_{\text{min}}^2/K)^{(L+1)}$ [10], where d_{min} is the minimum Euclidean distance between constellation points. Hence it follows that the maximum coding gain is given by $G_{c,\text{max}} = det(\mathbf{R}_h)^{1/(L+1)}d_{\text{min}}^2$. This shows that the proposed grouping scheme when $K \geq (L+1)$ allows for the same maximum coding gain as a full block size precoder. A much more rigorous proof than the one provided here has been shown in [8].

It is important to point out here, that so far we have not specified the kind of precoder needed to achieve the maximum diversity and coding gains. Such precoders have already been designed in [7]–[10] and in order to apply them to OCDM, $\mathbf{T}$ only needs to be a diagonal constellation rotation matrix.

V. Multiple Access

Downlink multiple access is fairly trivial and hence this paper focuses solely on the uplink, in which frequency selective channels cause the chirps to lose orthogonality resulting in inter user interference (IUI). This paper employs two different schemes to enable uplink multiple access and compares their performance.

A. FSP

We have already shown that FSP multiplexes multiple signals in the frequency domain while preserving the OCDM transmitter. Hence, here we simply extend it to a multi-user model and account for linear equalization.

Let us assume we have N_u users that are scheduled to transmit in one block duration. Furthermore, let us assume that each transmitter has M implemented branches, labeled in Fig. 1 as $\mathbf{u}_i \ \forall i \in [0, M-1]$, such that $M \geq N_u$. From this point on, we refer to these branches as resource blocks (RB). In order to simplify the analysis, we assume that the CP length is sufficient for all users. Modifying Eq. (13) for multi-user transmissions, the received signal at the m^{th} RB is given by

$$\hat{\mathbf{x}}_m = \mathbf{D}_{h,m}^{(u)} \mathbf{F}_K \mathbf{u}_m + \hat{\mathbf{n}}_m. \tag{19}$$

where $\mathbf{D}_{h,m}^{(u)}$ is a diagonal matrix with entries given by $[H^{(u)}(m),\ H^{(u)}(m+M),\ \dots,\ H^{(u)}(m+(K-1)M)]$. It is easy to see that linear equalizers can be implemented for each branch independently, denoted by $\mathbf{G}_m^{(u)}$, using either the zero forcing (ZF) or minimum mean squared error (MMSE) criterion. Thus, the equalized symbols for the m^{th} RB are given by

$$\hat{\mathbf{u}}_m = \mathbf{F}_K^{\mathcal{H}} \mathbf{G}_m^{(u)} \mathbf{D}_{h,m}^{(u)} \mathbf{F}_K \mathbf{u}_m + \mathbf{F}_K^{\mathcal{H}} \mathbf{G}_m^{(u)} \hat{\mathbf{n}}_m. \tag{20}$$

It is clear that each RB is processed individually at the receiver. Hence, there is no IUI and each RB can be independently modulated, e.g. use different constellations etc.

B. Joint detection

We adopt the second method from [6], originally proposed for multi-user detection and interference cancellation in doubly selective channels for OFDMA. We assume that there are N_u users that are scheduled to transmit such that $N_u \leq N$. Each user has been allocated a subset of chirps $\mathcal{R}_u$, which it uses to transmit data. Hence one example of an input sequence to the DFnT is given by $\mathbf{s}_u = [u_0,\ u_1,\ \dots,\ u_{|\mathcal{R}_u|-1},\ \mathbf{0}_{N-|\mathcal{R}_u|}^T]^T$. Modifying Eq. (2), the DFnT of a received block is given by

$$\hat{\mathbf{x}} = \mathbf{\Phi}\left(\sum_{u=1}^{N_u} \tilde{\mathbf{H}}^{(u)} \mathbf{\Phi}^{\mathcal{H}} \mathbf{J}_u \mathbf{u}_u + \mathbf{n}\right) = \sum_{u=1}^{N_u} \tilde{\mathbf{H}}^{(u)} \mathbf{J}_u \mathbf{u}_u + \mathbf{\Phi}\mathbf{n}, \tag{21}$$

where $\mathbf{u}_u$ is the u^{th} transmit block of size $|\mathcal{R}_u|$ and $\mathbf{J}_u$ is a zero padding $N \times |\mathcal{R}_u|$ matrix. Eq. (21) follows from the circular convolution property of the DFnT. Stacking the transmit vectors such that $\mathbf{r} = [\mathbf{u}_1^T,\ \dots,\ \mathbf{u}_{N_u}^T]^T$, we can form the equivalent model as

$$\hat{\mathbf{x}} = \underbrace{\left(\sum_{u=1}^{N_u} \tilde{\mathbf{H}}^{(u)} \mathbf{M}_u\right)}_{\mathbf{H}_{eq}} \mathbf{r} + \mathbf{\Phi}\mathbf{n}, \tag{22}$$

where $\mathbf{M}_u$ is an $N \times N$ matrix given by

$$M_u(m,n) = \begin{cases} 1 & \text{if } m = n \text{ and } m,n \in \mathcal{R}_u \\ 0 & \text{elsewhere.} \end{cases}$$

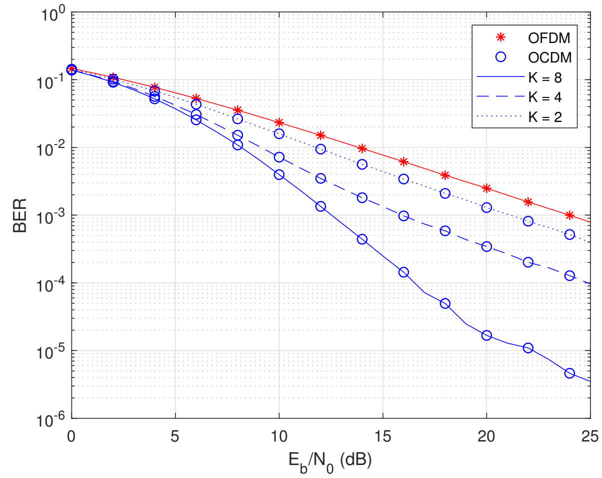

Fig. 2. Uncoded OCDM for different K and uncoded OFDM.

Using Eq. (22), it is easy to see that the formulation of an equivalent channel matrix $\mathbf{H}_{eq}$ mandates multi-tap equalization.

VI. Numerical Results

We simulate OCDM transmissions employing a QPSK constellation with $N = 8$ and vary K. The channel is quasi-static with a length of $L + 1 = 3$, the receiver has perfect channel state information (CSI), uses an MLE implemented through sphere decoding and the transmitter has no information about the channel. Results for full diversity GLCP-OFDM are shown for comparison. The constellation precoder for OCDM is given by $\mathbf{T} = diag(1,\ \alpha_1,\ \dots,\ \alpha_1^{K-1})$, where α_1 is defined in [7, Table 1].

Figure 2 shows the performance of OCDM without precoding for different values of K. The graph shows two important trends: Firstly, the BER slope seems to decrease as the SNR increases. This is more clear in the curve when $K = 8$ and occurs because the impact of errors with only one non-zero entry, i.e., the rank–1 blocks, is significantly larger at higher SNRs. A similar trend is observed for SC-CP transmissions in [11]. Secondly, decreasing K seems to adversely impact the performance, even when $K > L+1$. Due to the finite alphabet property, the probability of $\hat{\mathbf{e}}_{\mathbf{m}}$ having only one non-zero entry is an exponentially decreasing function of K. As a result, decreasing the block size leads to performance deterioration. However, it is pertinent to note that uncoded OCDM still shows better performance than uncoded OFDM.

Figure 3 shows the performance of precoded OCDM for different K. In agreement with the analysis in section IV, it can be seen that precoded OCDM offers full diversity and coding gains as long as $K \geq L + 1$. It is pertinent to note that the coded OFDM result shown for reference has been generated for $K = 4$. When $K < L + 1$, we can see a performance loss as the sub-blocks are not able to take full advantage of the channel. Combined with the constraint that $K = 2^l \ l \in \mathbb{Z}^+$, this presents an interesting tradeoff between complexity and

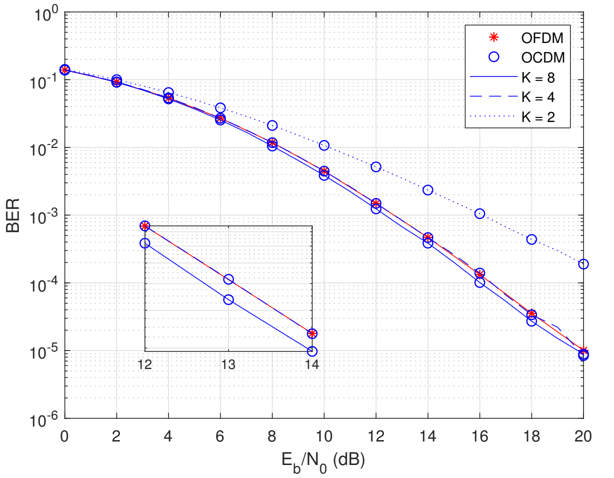

Fig. 3. LCP OCDM for different K and full diversity GLCP OFDM.

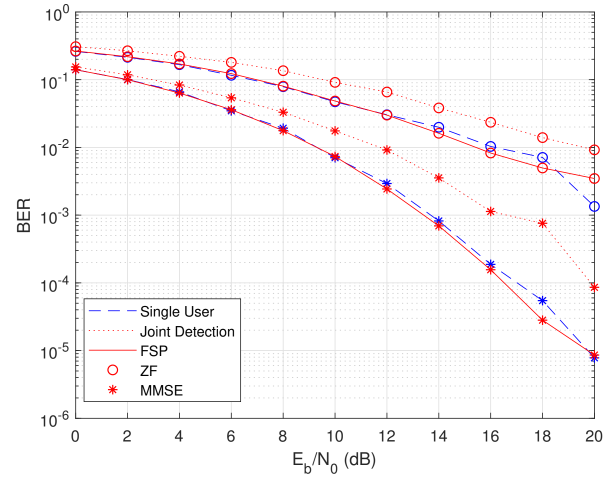

Fig. 4. Performance comparison of multi-user OCDM enabled through joint detection and FSP with single-user OCDM. For single user, $N = 64$ and for multiuser $|\mathcal{R}_u| = 64$.

performance. The graph also shows a marginal improvement for $K = 8$ in comparison to when $K = 4$. This trend was also noted in [7]–[8], and can be explained by the fact that the diversity and coding gains are just performance bounds and that other factors, like the kissing number, also impact BER performance.

Figure 4 compares the performance of the two multiple access schemes to single user OCDM. In this simulation the user block lengths $|\mathcal{R}_u|$ are kept equal to the total block length N in the single user case to avoid bias and an interleaved chirp allocation scheme is used in joint detection. It is clear that FSP preserves the performance of single user OCDM as the error rates for both are approximately the same. However, joint detection is limited by the interference caused by the loss of orthogonality in frequency selective channels. The RBs in FSP are designed so that orthogonality is preserved. Thus the performance of FSP is almost the same as that of the single user case.

VII. Conclusion

This paper proposed a novel symbol multiplexing technique to enable low complexity, high performance MLE and multiple access for OCDM. Furthermore, it introduces an alternative multiple access scheme for OCDM and compares the performance. It has been shown that using FSP, OCDM is possible to achieve the same performance as LCP OFDM. In addition, FSP enables low complexity linear FDE at the receiver for multi-user detection while maintaining the same performance as that of single user OCDM. However, there is an inherent trade-off between the implementation complexity and resource flexibility, i.e., is it better to have a large number of available RBs to allow for flexible allocation or is it better to limit this to lower transmitter design complexity?

In the near future, we plan on extending this work to incorporate channel estimation and techniques to reduce PAPR.

References

[1] X. Ouyang and J. Zhao, "Orthogonal chirp division multiplexing," *IEEE Trans. Commun.*, vol. 64, no. 9, pp. 3946-3957, Sept. 2016.

[2] X. Ouyang and J. Zhao, "Orthogonal Chirp Division Multiplexing for Coherent Optical Fiber Communications," *J. Lightw. Technol.*, vol. 34, no. 18, pp. 4376-4386, Sept.15, 2016.

[3] X. Ouyang, G. Tall, M. Power and P. Townsend, "Experimental demonstration of 112 Gbit/s orthogonal chirp–division multiplexing based on digital up-conversion for IM/DD systems with improved resilience to system impairments," *Eur. Conf. on Opt. Commun.*, Rome, 2018, pp. 1-3.

[4] F. Lu, L. Cheng, M. Xu, J. Wang, S. Shen, and G. K. Chang, "Orthogonal chirp division multiplexing in millimeter-wave fiber-wireless integrated systems for enhanced mobile broadband and ultra-reliable communications," in *Proc. Optical Fiber Commun. Conf.,* Los Angeles, CA, 2017, pp. 1-3.

[5] X. Ouyang, O. A. Dobre, Y. L. Guan and J. Zhao, "Chirp spread spectrum toward the nyquist signaling rate–orthogonality condition and applications," *IEEE Signal Process. Lett.,* vol. 24, no. 10, pp. 1488-1492, Oct. 2017.

[6] S. Hou and C. C. Ko, "Intercarrier Interference Suppression for OFDMA Uplink in Time- and Frequency-Selective Fading Channels," *IEEE Trans. Veh. Technol.,* vol. 58, no. 6, pp. 2741-2754, Jul. 2009.

[7] Z. Liu, Y. Xin, and G. B. Giannakis, "Linear constellation precoding for OFDM with maximum multipath diversity and coding gains," *IEEE Trans. Commun.*, vol. 51, no. 3, pp. 416-427, Mar. 2003.

[8] N. H. Tran, H. H. Nguyen, and T. Le-Ngoc, "Subcarrier Grouping for OFDM With Linear Constellation Precoding Over Multipath Fading Channels," *IEEE Trans. Veh. Technol.,* vol. 56, no. 6, pp. 3607-3613, Sept. 2007.

[9] S. Zhou and G. B. Giannakis, "Single-carrier space-time block-coded transmissions over frequency-selective fading channels," *IEEE Trans. Inf. Theory,* vol. 49, no. 1, pp. 164-179, Jan. 2003.

[10] Y. Xin, Z. Wang, and G. B. Giannakis, "Space-time diversity systems based on linear constellation precoding," *IEEE Trans. on Wireless Commun.,* vol. 2, no. 2, pp. 294-309, Mar. 2003.

[11] M. Ghogho, V. P. Gil-Jimenez, and A. Swami, "Multipath diversity and coding gains of cyclic-prefixed single carrier systems," in *Proc. Int. Conf. Acoustics, Speech and Signal Processing*, Taipei, 2009, pp. 2837-2840.

[12] Z. Wang, and G. B. Giannakis, "Wireless multicarrier communications," *IEEE Sig. Process. Mag.,* vol. 17, no. 3, pp. 29-48, May 2000.

[13] A. Berman and N. Shaked-Monderer, *Completely Positive Matrices. Singapore*, World Scientific, 2003.

[14] U. Sorger, I. D. Broeck, and M. Schnell, "Interleaved FDMA-a new spread-spectrum multiple-access scheme," in *Proc. Int. Conf. Commun.,* Atlanta, GA, 1998, pp. 1013-1017 vol. 2.